A Subspace Based Approach to Pulse Design with Application to UWB Communications

S. Chandan, P. Sandeep and A. K. Chaturvedi, *Senior Member, IEEE*
Department of Electrical Engineering
Indian Institute of Technology Kanpur
India
Email: {csaurabh, sandeepp, akc}@iitk.ac.in

***Abstract*— In UWB systems, FCC mask puts a constraint on the Maximum Allowable Transmit Power (MATP) of a pulse. The transmit power of a pulse is an important parameter that determines the BER performance and range. In this paper a subspace based approach has been found to make the MATP optimization easier which otherwise seems intractable due to mask constraints. The design procedure begins with some pulse width and then we optimize for MATP. The obtained pulses turn out to have higher MATP than the known pulses of the same width. We show that using the proposed pulses, a lower BER than that of the existing pulses can be achieved. The proposed approach is applicable to the FCC mask or any other piecewise constant mask that may be proposed in future.**

I. Introduction

Recently there has been a spate of research in the area of pulse design in general, as well as for UWB applications [1], [2], [3]. In a UWB system, the choice of pulse shape strongly affects the design of transceiver as well as the bit error performance. Gaussian monocycles were initially proposed and are being widely used for UWB applications [4]. In the light of [5], pulses for UWB need not be constrained to some standard shapes like Gaussian monocycles and its derivatives. Hence, it is possible to consider new approaches to pulse design for UWB applications. A pulse designed for UWB should have a small pulse width and it should fit the FCC mask [4]. Recently, new pulse families have been proposed which were shown to fit the FCC mask criterion [3], [6], [7], [8].

Apart from mask fitting, the pulses should also have other desirable characteristics. It is well known that the BER performance of a pulse depends on the transmitted power. It was shown in [6] and [7] that the pulse shape puts a constraint on the maximum allowable transmit power that could be transmitted without violating the FCC mask. We refer to this Maximum Allowable Transmit Power as the MATP of that pulse. References [6] and [7] have tried to optimize pulses based on Gaussian monocycles for MATP subject to FCC mask constraint. However, these pulse designs for increased MATP resulted in increase of pulse width which is undesirable for high data rate applications [6], [7]. Hence, it is desired to examine whether it is possible to have pulses with higher transmit power than the existing pulses without compromising on pulse width.

In this paper we design pulses for a given pulse width that not only fit the FCC mask but also have more MATP than the contemporary pulses of same width. We also show that for a fixed data rate, a lower BER than that of the existing pulses can be achieved using the proposed pulses. Further, using the proposed design procedure, pulses can be designed for any piecewise constant mask.

The paper is organized as follows. In the next section we discuss some preliminaries and highlight the importance of MATP in UWB communications. Section III discusses the new design approach. In Section IV, design examples are given to illustrate the usefulness of the proposed family. Finally, Section V summarizes the results obtained.

II. Preliminaries

Several modulation techniques have been proposed for UWB communications. In schemes such as Biphase Modulation (BPM) , On-Off Keying, Time-Hopping Binary Phase Shift Keying, Time-Hopping Pulse Position Modulation and Pulse Position Modulation, transmit power of the pulse plays an important role in deciding the BER performance [4], [9]. For example, for BPM, the BER is given by [10]

$$P_e = Q\left(\sqrt{\frac{2E_r}{N_o}}\right) \tag{1}$$

where E_r is the received energy per bit and $N_o/2$ is the double sided PSD of Additive White Gaussian Noise (AWGN). Let T_b be the bit interval. If α is the attenuation factor, then the received energy per bit is directly proportional to the transmitted energy per bit E_t and is given by $E_r = \alpha^2 E_t$. Then the received power is given by $P_r = E_r/T_b = \alpha^2 P_t$ where P_t is the transmitted power. The SNR at the receiver is given by $E_r/N_o = \alpha^2 E_t/N_o = \alpha^2 P_t T_b/N_o$. Now, because of the need to satisfy the FCC mask, any arbitrary amount of power cannot be transmitted and hence maximum value of P_t, i.e. MATP, is fixed for a pulse. So, for a given noise power and T_b, arbitrarily high values of SNR cannot be achieved. Further, from (1), it is clear that BER depends on SNR. Thus for a pulse with a given MATP, the upper bound on SNR puts a limit on the minimum achievable BER. It is important to note that even otherwise, pulses with high transmit power can find applications in environments with high noise power and/or for transmitting over longer ranges.

1-4244-0355-3/06/$20.00 (c) 2006 IEEE

This full text paper was peer reviewed at the direction of IEEE Communications Society subject matter experts for publication in the IEEE ICC 2006 proceedings.

III. Design Approach

In the context of UWB, a pulse can be useful only if its Power Spectral Density (PSD) lies within the FCC Mask. Since the FCC mask is defined in the frequency domain, we propose a frequency domain approach to pulse design. One of the limitations of such an approach is that the pulse designed cannot be ensured to be limited in time. This limitation can be overcome by designing pulses that are highly concentrated in a given time interval and then truncating them. The measure of concentration, μ, of a bandlimited function $h(t)$ in the time interval $|t| \leq T/2$ has been defined as [11]

$$\mu = \frac{\int_{-T/2}^{T/2} h^2(t)dt}{\int_{-\infty}^{\infty} h^2(t)dt} \tag{2}$$

A higher μ for a pulse implies a higher concentration in time.

Another issue is the maximization of MATP over the space of all bandlimited pulses. It becomes complicated by the constraint that the resulting pulse has to satisfy the mask. In this paper we show that a subspace based approach leads to a convenient solution to this problem. In this approach, the MATP is maximized over a subspace of bandlimited pulses. We try to find a basis for this subspace of the space of bandlimited functions (defined later). We show that the members of this basis with high values of μ can be linearly combined so that the resulting pulse can be optimized for MATP subject to mask constraints. We find that it is possible to truncate these pulses such that the PSD of the truncated pulse also satisfies the mask. In [14], a basis was found for the space of bandlimited functions. We point out towards the end of Section III that the basis derived in [14] is of limited utility to the problem at hand.

A. Subspace of Bandlimited functions

Let us consider a function $P(f)$ which is real and bandlimited in $[f_L, f_H]$ where $0 \leq f_L < f_H$. The set $\mathcal{F} = [f_1, \cdots, f_n]$ represents a set of frequencies between f_L and f_H. To get a subspace of the space of bandlimited functions, $\mathcal{B}$, we define a linear transformation Γ on $P(f)$ such that

$$\Gamma[P(f)] = \sqrt{T_b} \sum_{i=1}^{n} P(f_i) D_i(f) \tag{3}$$

where $D_i(f)$ is given by

$$D_i(f) = \begin{cases} \Psi\left(\frac{f-f_i}{f_{i+1}-f_i}\right) & f_i \leq f \leq f_{i+1} \\ \Psi\left(\frac{f_i-f}{f_i-f_{i-1}}\right) & f_{i-1} \leq f \leq f_i \end{cases} \tag{4}$$

Also, $f_0 = f_L$, $f_{n+1} = f_H$ and $\Psi(f)$ is any function bandlimited in the interval $[0,1]$ with $\Psi(0) = 1$ and $\Psi(1) = 0$. This form of $\Psi(f)$ makes $\Gamma[P(f_i)] = \sqrt{T_b} P(f_i)$ which simplifies further analysis. Now, using $\Gamma[P(f)]$, we can form a real even pulse $g_e(t)$ and a real odd pulse $g_o(t)$. The respective Fourier transforms $G_e(f)$ and $G_o(f)$ are defined by

$$\begin{aligned} G_e(f) &= \Gamma[P(f)] + \Gamma[P(-f)] \\ G_o(f) &= j(\Gamma[P(f)] - \Gamma[P(-f)]) \end{aligned} \tag{5}$$

The sets of even and odd pulses form subspaces W_e and W_o of $\mathcal{B}$. We want to find the functions in W_e and W_o which have the largest value of μ as defined by (2).

B. Most concentrated pulse

We first find a simplified expression of concentration for pulses in W_e. Since the design is in frequency domain, we try to express (2) in terms of $G_e(f)$. Using the inverse Fourier transform expression $g_e(t) = 2\int_{f_L}^{f_H} G_e(f)\cos(2\pi ft)df$ in the numerator and using Parseval's theorem in the denominator of (2), μ can be expressed as

$$\mu = \frac{4\int_{-T/2}^{T/2}\int_{f_L}^{f_H}\int_{f_L}^{f_H} G_e(f_x)G_e(f_y)\zeta(f_x,f_y,t)df_x df_y dt}{2\int_{f_L}^{f_H}|G_e(f)|^2 df} \tag{6}$$

where $\zeta(f_x, f_y, t) = \cos(2\pi f_x t)\cos(2\pi f_y t)$. Interchanging the order of integrals and evaluating the integral with respect to t, we get

$$\mu = \frac{T\int_{f_L}^{f_H}\int_{f_L}^{f_H} G_e(f_x)G_e(f_y)\rho(f_x,f_y)df_x df_y}{\int_{f_L}^{f_H}|G_e(f)|^2 df} \tag{7}$$

where $\rho(f_x, f_y)$ is given by

$$\rho(f_x, f_y) = \text{sinc}(T(f_x+f_y) + \text{sinc}(T(f_x-f_y)) \tag{8}$$

Now, substituting (3) in (5) and $G_e(f)$ from (5) into (7), we get

$$\mu(\mathbf{p}) = \frac{\mathbf{p}^t A\mathbf{p}}{\mathbf{p}^t C\mathbf{p}} \tag{9}$$

where $A = [a_{ij}]_{n\times n}$, $\mathbf{p} = [P(f_1), \cdots, P(f_n)]^t \in \Re^{n\times 1}$ and $C = [c_{ij}]_{n\times n}$. We refer to $\mathbf{p}$ as the pulse vector. Bold representation is used for vectors. The entries in A and C are given by

$$\begin{aligned} a_{ij} &= T\int_{f_L}^{f_H}\int_{f_L}^{f_H} D_i(f_x)D_j(f_y)\rho(f_x,f_y)df_x df_y \\ c_{ij} &= \int_{f_L}^{f_H} D_i(f)D_j(f)df \end{aligned}$$

It can be shown that for $g_o(t) \in W_o$, $\mu(\mathbf{p})$ can be expressed as in (9) with $\rho(f_x, f_y)$ given by

$$\rho(f_x, f_y) = \text{sinc}(T(f_x-f_y)) - \text{sinc}(T(f_x+f_y)) \tag{10}$$

Thus, by choosing $\rho(f_x, f_y)$ from (8) or (10), (9) defines concentration for pulses belonging to W_e or W_o respectively. Let $g(t)$ be a pulse belonging to W_e or W_o with Fourier transform $G(f)$. Then its concentration is given by (9) where $\mathbf{p}$ is the corresponding pulse vector of $G(f)$.

The ratio in (9) is popularly known as the Rayleigh Quotient of the matrices A and C and its maxima or minima occur when the gradient $\nabla\mu(\mathbf{p}) = 0$ [12]. The gradient of (9) is given by

$$\nabla\mu(\mathbf{p}) = \frac{2}{\mathbf{p}^t C\mathbf{p}}[A - \mu(\mathbf{p})C]\mathbf{p} \tag{11}$$

Therefore, the maxima or minima occur at

$$A\mathbf{p} = \lambda C\mathbf{p} \tag{12}$$

$$g_e(t) = 2\sqrt{T_b}\sum_{i=1}^{n} P(f_i)\ \mathrm{Re}\left[e^{j2\pi f_i t}\left\{(f_{i+1}-f_i)\psi(t(f_{i+1}-f_i)) + (f_i - f_{i-1})\psi(t(f_{i-1}-f_i))\right\}\right] \quad (15)$$

$$g_o(t) = -2\sqrt{T_b}\sum_{i=1}^{n} P(f_i)\ \mathrm{Im}\left[e^{j2\pi f_i t}\left\{(f_{i+1}-f_i)\psi(t(f_{i+1}-f_i)) + (f_i - f_{i-1})\psi(t(f_{i-1}-f_i))\right\}\right] \quad (16)$$

The solutions of (12), $\{(\mathbf{p}_i, \lambda_i)\}$, are generalized eigenvectors and eigenvalues of the matrices A and C. We denote the pulses corresponding to these eigenvectors as the eigenpulses $g_i(t)$ with Fourier transform $G_i(f)$. As is clear from (12), the eigenvalues denote the concentration of the eigenpulse corresponding to eigenvector $\mathbf{p_i}$ and hence a high λ_i implies high concentration of that eigenpulse in time. The eigenpulse corresponding to pulse vector $\mathbf{p}$ with the largest eigenvalue is the most concentrated in time $[-T/2, T/2]$ for the space of W_e or W_o.

C. Basis of Eigenpulses

We show that the eigenpulses form the basis of the subspaces W_e or W_o depending upon the choice of $\rho(f_x, f_y)$ from (8) or (10) respectively. As $\mathbf{p}^t C\mathbf{p} = \frac{1}{T_b}\int_{f_L}^{f_H} |G(f)|^2 df > 0$ for any $\mathbf{p}$, hence C is positive definite. By Cholesky decomposition, C can be expressed as $C = LL^t$, where L is an invertible matrix [12]. Substituting $C = LL^t$ in (12) and pre-multiplying by L^{-1}, we get

$$(L^{-1}A(L^t)^{-1})(L^t\mathbf{p}) = \lambda L^t\mathbf{p}$$

Thus $L^t\mathbf{p}$ is the eigenvector of $(L^{-1}A(L^t)^{-1})$ for eigenvalue λ. Using $(L^t)^{-1} = (L^{-1})^t$, $(L^{-1}A(L^t)^{-1}) = (L^{-1}A(L^{-1})^t)$. Since $(L^{-1}A(L^{-1})^t)$ is real and symmetric hence $L^t\mathbf{p}$ spans $\Re^{n\times 1}$ [12]. Since L^t is invertible hence the set of eigenvectors $\{\mathbf{p}_i\}$ also spans $\Re^{n\times 1}$. So (12) has n independent eigenvectors given by $\{\mathbf{p}_i\}, i = 1, \cdots, n$.

For the eigenpulses $\{G_i(f)\}$ to form a basis, we show that all the eigenpulses are linearly independent and that they span their corresponding subspace W_e or W_o.

Lemma 1: The set of eigenpulses $\{G_i(f)\}$ corresponding to independent eigenvectors $\{\mathbf{p_i}\}$ is linearly independent.

Proof: Since $\{\mathbf{p_i}\}$ forms a set of linearly independent vectors, it implies that if $\sum_i x_i\mathbf{p_i} = 0$ then all $x_i = 0$. Consider,

$$\sum_i x_i G_i(f) = 0 \qquad \forall f$$

Using (3) and (5) in the above equation, we get for W_e

$$\left(\sum_i x_i\mathbf{p_i}\right)\cdot \mathbf{d}(f) + \left(\sum_i x_i\mathbf{p_i}\right)\cdot \mathbf{d}(-f) = 0 \quad (13)$$

and for W_o

$$j\left(\left(\sum_i x_i\mathbf{p_i}\right)\cdot \mathbf{d}(f) - \left(\sum_i x_i\mathbf{p_i}\right)\cdot \mathbf{d}(-f)\right) = 0 \quad (14)$$

where $\mathbf{d}(f) = [D_1(f), D_2(f), \cdots, D_n(f)]^t$ and dot product $\mathbf{a}\cdot\mathbf{b} = a^t b$. For $f > 0$, both (13) and (14) become

$$\left(\sum_i x_i\mathbf{p_i}\right)\cdot \mathbf{d}(f) = 0$$

This is true only if $(\sum_i x_i\mathbf{p_i}) = 0$. Since $\{\mathbf{p_i}\}$ is an independent set, this implies all $x_i = 0$. This implies that $G_i(f)$ are independent. ∎

It can be easily seen from (3) and (5) that W_e and W_o are n dimensional subspaces. Since eigenpulses $G_i(f)$ corresponding to the eigenvectors of (12) form a set of n independent pulses in W_o or W_e, they form a basis of W_o or W_e respectively.

From the above discussion, we have been able to obtain a set of eigenpulses that span the subspace of even or odd bandlimited pulses. Moreover, these pulses are bandlimited and can be ordered according to their energy concentration as defined by (2). In subsequent sections, we use these eigenpulses to obtain pulses with desired characteristics.

Time domain expression of the resulting pulse $g_e(t)$ and $g_o(t)$ are given in (15) and (16) respectively where $\psi(t)$ is the inverse Fourier transform of $\Psi(f)$ and $\mathrm{Re}(\cdot)$ and $\mathrm{Im}(\cdot)$ represents the real and imaginary parts respectively.

D. Linear Combination of Eigenpulses

The individual eigenpulses that are highly concentrated in time, i.e. λ close to 1, may not have high MATP. Hence, we consider the linear combination of eigenpulses to obtain pulses maximized for MATP. As shown by the following lemma, the concentration of the linear combination of eigenpulses can be ensured to be greater than λ if the eigenpulses with concentration greater than λ are considered for the combination.

Lemma 2: The concentration of the linear combination of eigenpulses is lower bounded by the minimum eigenvalue of the constituent eigenpulses.

Proof: Let us consider the linear combination of m ordered eigenpulses with generalized eigenvalues $\{\lambda_1, \cdots, \lambda_m\}$. Then the linear combination of the eigenvectors is given as $\mathbf{p} = V\mathbf{a}$, where $V = [\mathbf{p_1}\cdots\mathbf{p_m}]$ represents the eigenvectors used for linear combination. The vector containing the coefficients used in the linear combination is $\mathbf{a} = [a_1, \cdots, a_m]^t$. Substituting $\mathbf{p} = V\mathbf{a}$ in (9), we get $\mu = \frac{\mathbf{a}^t V^t AV\mathbf{a}}{\mathbf{a}^t V^t CV\mathbf{a}}$. The maximum and minimum values of μ occur when the gradient of μ equals zero. The gradient can be found as in (11) and consequently the maximum and minimum values of μ occur at eigenvectors with maximum and minimum eigenvalues of the matrices (V^tAV, V^tCV). It can be seen that the eigenvalues of (V^tAV, V^tCV) are $\lambda_k, k = \{1, \cdots, m\}$ with the

TABLE I

EIGENVALUES OBTAINED FOR W_e AND W_o

$T = 0.46$ns		$T = 1.0$ns	
Even	Odd	Even	Odd
$1.0000e-0$	$1.0000e-0$	$1.0000e-0$	$1.0000e-0$
$9.9995e-1$	$9.9997e-1$	$9.9998e-1$	$9.9998e-1$
$9.9953e-1$	$9.9909e-1$	$9.9993e-1$	$9.9993e-1$
$9.8773e-1$	$9.8377e-1$	$9.9980e-1$	$9.9980e-1$
$7.9664e-1$	$8.9746e-1$	$9.9953e-1$	$9.9956e-1$
$5.6262e-1$	$3.2219e-1$	$9.9903e-1$	$9.9905e-1$
$5.6829e-2$	$1.4458e-2$	$9.9817e-1$	$9.9826e-1$
$8.4345e-3$	$6.2616e-3$	$9.9667e-1$	$9.9671e-1$
$5.1222e-4$	$6.0798e-5$	$9.9417e-1$	$9.9468e-1$
$3.4947e-6$	$3.0567e-7$	$9.8741e-1$	$9.7995e-1$

TABLE II

TRADE-OFF BETWEEN PULSE WIDTH AND MATP FOR W_e

T in ns	Number of eigenpulses	$MATP_s$ in mW	$MATP_p$ in mW
0.35	2	0.575	0.327
0.46	3	0.601	0.461
	4	0.846	
0.60	4	0.772	0.417
	5	0.822	
	6	0.865	
	7	0.866	
0.80	6	0.886	0.440
	7	0.926	
	8	0.928	
1.00	7	0.910	0.336
	8	0.935	
	9	0.940	

corresponding eigenvectors as $\mathbf{a_k} = [\alpha_{ij}]_{n\times 1}$ where $\alpha_{ij} = 1$ if $(i,j) = (k,1)$ and $\alpha_{ij} = 0$ otherwise. ∎

E. Mask Fitting

Another aspect of design is that the linear combination of eigenpulses has to fit the FCC mask. In (3), if an additional condition is imposed that $\Psi(f)$ is a monotonic function and $\Psi(f) = 1 - \Psi(1-f)$ then it can be easily observed from (3) and (5) that $G_e(f)$ and $G_o(f)/j$ become piecewise monotonic functions. This means that in any given interval (f_i, f_{i+1}), they are either increasing or decreasing. Let us assume that the mask is piecewise constant which is true for the case of FCC mask. Also, let $\mathcal{F}$ necessarily include all the points where the mask is discontinuous and some additional points for more flexibility in design. Then ensuring that $|G(f_i)|^2/T_b$ for all $f_i \in \mathcal{F}$ lie at or below the mask also ensures that $|G(f)|^2/T_b$ lies at or below the mask for all frequencies. Thus the mask constraints on PSD are given by $\frac{|G(f_i)|^2}{T_b} \leq M(f_i), f_i \in \mathcal{F}$ where $M(f)$ represents the mask on PSD. Equivalently, using $\Gamma[P(f_i)] = \sqrt{T_b}P(f_i)$ and (5), the constraints can be written as $|P(f_i)|^2 \leq M(f_i), f_i \in \mathcal{F}$. Hence, using $\mathbf{p} = V\mathbf{a}$, the constraints in terms of $\mathbf{a}$ are given by

$$-\mathbf{s} \leq V\mathbf{a} \leq \mathbf{s} \tag{17}$$

where V is the matrix of chosen eigenvectors and $\mathbf{s} = [\sqrt{M(f_1)}, \cdots, \sqrt{M(f_n)}]$. Thus it can be observed that the selection of the subspace (3) has reduced the mask fitting constraint to a set of finite number of linear inequalities.

F. Optimization

The linear combination of eigenpulses can be easily optimized for MATP. From Section III.A, the transmit power of the truncated pulse is $\frac{1}{T_b}\int_{-T/2}^{T/2} g^2(t)dt = 2\mathbf{p}^t A\mathbf{p}$. Then, by using $\mathbf{p} = V\mathbf{a}$, the optimization problem can be written as

$$\begin{aligned} \text{maximize} \quad & 2\mathbf{a^t}V^tAV\mathbf{a} \\ \text{subject to} \quad & -\mathbf{s} \leq V\mathbf{a} \leq \mathbf{s} \end{aligned} \tag{18}$$

Since A is positive definite, $(V\mathbf{a})^tA(V\mathbf{a}) > 0$, hence V^tAV is also a positive definite matrix. Hence, $2\mathbf{a^t}V^tAV\mathbf{a}$ is a convex function in $\mathbf{a}$. We show in Appendix that the inequalities in (18) define a bounded polyhedron. So, the problem is to maximize a convex function in a bounded polyhedron and hence, the maximum will occur at one of the vertices of the polyhedron [13]. The vertices of the polyhedron defined by the inequalities can be found using Vertex Enumeration for Convex Polytopes and Arrangements Package of MATHEMATICA. The function $(2\mathbf{a^t}V^tAV\mathbf{a})$ is then evaluated at all the vertices obtained and the vertex with the maximum value of function is the desired solution.

In [14], a basis of the space of bandlimited functions was derived and the first few basis members were shown to be highly concentrated in time. However, considering their linear combination for optimization of MATP seems intractable as it leads to an infinite number of mask constraints. This is because, while optimization, we will have to ensure that the linear combination lies at or below the mask at every frequency value in contrast to a finite number of frequency values for the subspace based approach.

IV. DESIGN EXAMPLES

Using the discussed approach, pulses can be designed for any mask that is piecewise constant. Hence, we can design pulses that satisfy the indoor FCC mask or those that satisfy the outdoor FCC mask [4]. In this paper we design pulses for the indoor FCC mask. The vector $\mathcal{F}$ considered is

$$\mathcal{F} = \{f_k | f_k = 2.6 + 0.5(k-1), k = 1, \cdots, 23\} GHz \tag{19}$$

Also, let f_L = 2.1GHz and f_H = 14.1GHz so that the pulse (untruncated) obtained is bandlimited between 2.1GHz to 14.1GHz. This choice of f_L and f_H includes the band $[3.1, 10.6]$GHz where FCC has allowed a higher PSD. More points in $\mathcal{F}$ provide better design at the cost of computational complexity. For illustration, we consider $\Psi(f)$ to be $(1-f)$ $\forall f \in [0,1]$. Then, using (12) we can compute the generalized eigenvalues and generalized eigenvectors of the matrices (A, C) for values of pulse width T. The time domain expression of the pulse $g(t)$ can be found by substituting $\psi(t)$ and the corresponding pulse vector in (15) or (16) where $\psi(t)$

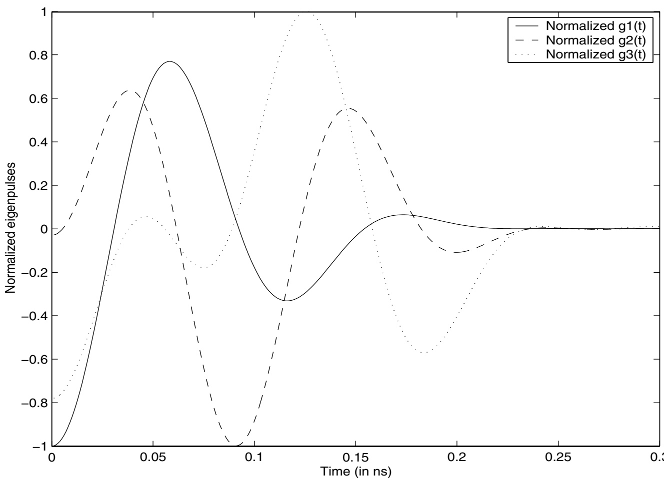

Fig. 1. First three normalized eigenpulses for $T = 0.46$ns

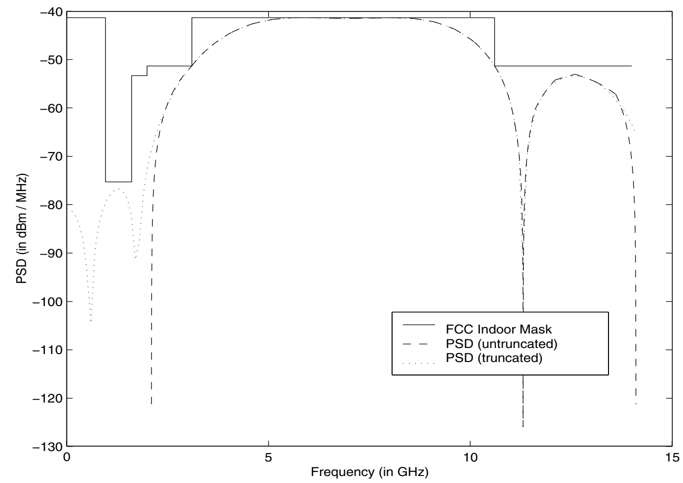

Fig. 2. PSD of the pulse shape designed by linearly combining first four ordered eigenvectors for $T = 0.46$ns

is given by

$$\psi(t) = \frac{1}{2}\ \text{sinc}^2(t) - \frac{j}{2\pi t}(1 + \ \text{sinc}(2t)) \qquad (20)$$

Table I gives the eigenvalues obtained for two different values of T, 0.46ns and 1.0ns, both for W_e and W_o. Only the first 10 ordered eigenvalues are shown. It can be re-emphasized that by choosing $\rho(\cdot,\cdot)$ from (8) or (10), we can choose the pulse to be even or odd respectively. After truncation, the designed pulse is likely to fit the mask if it is highly concentrated in time $[-T/2, T/2]$. Lemma 2 shows that the concentration of the designed pulse is lower bounded by the minimum eigenvalue of its constituent eigenpulses. Hence it is desirable to combine eigenpulses with high concentration, μ.

As can be noted from the table, the first few eigenvalues are close to 1 implying that the corresponding eigenpulses are highly concentrated in time $[-T/2, T/2]$. It can be noted that the eigenvalues become significantly small after the first few. This behaviour is similar to that observed in [14]. Also, the number of eigenvectors with eigenvalues close to 1 is more for $T = 1.0$ns than when $T = 0.46$ns. This implies that for a higher pulse width T, we have more vectors that can be combined and hence more flexibility in design as the eigenpulses are linearly independent (Lemma 1). For $T = 0.46$ns, normalized eigenpulses, $g_i(t)/\max(|g_i(t)|)$, for the first three eigenvalues are shown in Fig. 1. Here, $\max(|g_i(t)|)$ represents the maximum value of $|g_i(t)|$. The high concentration of the first three eigenpulses as shown in Table I can be corroborated by Fig. 1.

A. Comparisons

Table II shows the MATP of the designed pulses for different pulse widths along with the number of eigenpulses used for linear combination. All the pulses shown in the table have a concentration $\mu > 99.9\%$ and satisfy the FCC mask after truncation to $[-T/2, T/2]$. The values of MATP shown in the table are for pulses truncated to $[-T/2, T/2]$. For a

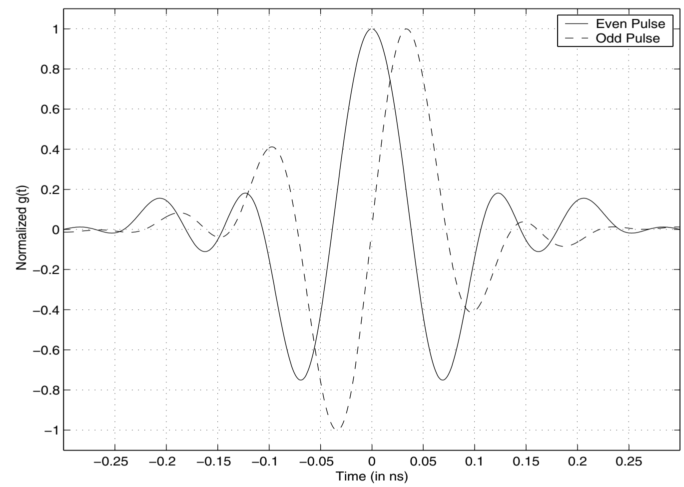

Fig. 3. Time domain of normalized pulse shapes designed by linearly combining first four ordered eigenvectors for $T = 0.46$ns

given T, it can be observed that the MATP is higher when more number of eigenpulses are linearly combined. We have shown the comparisons for even pulses. Similar results hold for odd pulses also. The obtained results are compared with the Prolate Spheroidal pulses (PS) [8] for the same values of T. In [8], multiple pulses can be designed for a given T. In Table II, $MATP_p$ is the maximum MATP obtained from all the PS pulses that can be designed for the given T. It can be seen that the new pulses outperform the PS pulses in MATP. The performance of subspace based pulses is also better than that of the popularly used Gaussian 4^{th} and 5^{th} monocycles [9], [6]. Both these pulses have pulse width $T = 0.46$ns. The MATP of Gaussian 4^{th} monocycle is 0.629mW and that of Gaussian 5^{th} monocycle is 0.482mW. Newly designed pulse has a higher MATP of 0.846mW for the same pulse width.

We can also observe that as T for the proposed pulses increases, MATP increases. However, the potentially achievable maximum data rate, R_{max}, decreases with increase in T. Thus, there exists a trade-off between MATP and R_{max}. Attempts to get pulses with more MATP have been done in [6], [7]. The pulse designed for FCC mask in [6] has an MATP of 0.560mW and 0.6ns pulse width. The subspace based design approach allows us to achieve a higher MATP of 0.866mW for the same pulse width. In [7], for a pulse width of 1.3ns, the MATP obtained was 0.910mW. We have obtained a higher MATP of 0.940mW for a lower pulse width of 1.0ns by combining the first 9 ordered eigenpulses. Recently, in [3], pulses have been designed for UWB using B-Spline functions. The MATP of these pulses, referred to as B-Spline pulses, are 0.213mW and 0.281mW and the pulse width is 1.6ns. As is clear from Table II, our approach yields pulses with much higher MATP even at lower pulse widths. It can be noted that unlike the proposed approach, none of the design procedures in [6], [3] give the freedom to decide the pulse width while designing. However, in [3] and [8], multiple orthogonal pulses can be designed.

Fig. 2 depicts the PSD of the untruncated even pulse designed for $T = 0.46$ns by combining the first four ordered eigenpulses as given in Table II, along with the FCC mask. Also shown is the PSD of this pulse when truncated in $[-0.23, 0.23]$ns. It can be easily observed that the PSD of the truncated pulse is below the FCC mask. This can be attributed to the high concentration of the untruncated pulse in $[-0.23, 0.23]$ns. Fig. 3 shows the normalized even and odd pulses, $g(t)/\max(|g(t)|)$, designed for $T = 0.46$ns by combining the first four ordered eigenpulses. It should be noted that even and odd pulses are orthogonal and hence can be used for increasing the data rate of the same user.

The BER for BPM as given in (1) can also be expressed in terms of transmit power P_t as

$$P_e = Q\left(\sqrt{\frac{2\alpha^2 T_b P_t}{N_o}}\right)$$

For a given T_b, N_o and α^2, the lower bound on P_e for a particular pulse can be obtained by replacing P_t with MATP of that pulse. If different pulses are transmitted at the same data rate $1/T_b$ and under same transmission conditions, that is, same α and N_o, then it is evident from the BER expression that since proposed pulses have higher MATP, they will have a lower BER.

V. Conclusion

In this paper we have proposed a subspace based approach to pulse design with applications to UWB. A subspace of bandlimited functions has been found to make the MATP optimization easier, which otherwise seems intractable due to mask constraints. We find a basis to this subspace and choose the members of the basis which are concentrated in time. Linear combination of these members is optimized for MATP subject to mask constraints. The obtained pulses have been found to have higher MATP than the existing pulses for the same pulse width. It is observed that for the subspace considered, there exists a tradeoff between the pulse width and MATP. We also show that for a fixed data rate, a lower BER than that of the existing pulses can be achieved using the proposed pulses. The proposed approach is applicable to the FCC mask or any other piecewise constant mask that may be proposed in future.

References

[1] S. Chandan, P. Sandeep and A. K. Chaturvedi, *"A family of ISI-free polynomial pulses"*, IEEE Commun. Lett., Vol 9, pp. 496-498, Jun 2005.

[2] N. C. Beaulieu and M. O. Damen *"Parametric construction of Nyquist-I pulses"*, IEEE Trans. Commun., Vol 52, pp. 2134-2142, Dec. 2004.

[3] Y. Kim, B. Jang, C. Shin and B. F. Womack, *"Orthonormal Pulses for High Data Rate Communications in Indoor UWB Systems"*, IEEE Commun.Lett., vol. 9, pp. 405-407, May 2005.

[4] M. Ghavami, L. B. Michael and R. Kohno, *Ultra Wideband Signals and Systems in Communication Engineering* , John Wiley, England, 2004.

[5] I. S. Lin, J. D. McKinney and A. M. Weiner, *"Photonic Synthesis of Broadband Microwave Arbitrary Waveforms Applicable to Ultra-Wideband Communication"*, IEEE Microw. Wireless Compon. Lett., vol. 15, pp. 226-228, Apr. 2005.

[6] Y. Wu, F. S. Molisch, S.Y. Kung, J. Zhang, *"Impulse Radio Pulse Shaping for Ultra-Wide Bandwidth (UWB) Systems"* , IEEE PIMRC-2003, Vol. 14, pp. 877-881, 2003.

[7] X. Luo, L. Yang and G. B. Giannakis, *"Designing Optimal Pulse-Shapers for Ultra-Wideband Radios"* , IEEE Conference on Ultra Wideband Systems and Technologies, 16-19 Nov. 2003, pp. 349-353, 2003

[8] B. Parr, B. Cho, K. Wallace and Z. Ding, *"A Novel Ultra-Wideband Pulse Design Algorithm"* , IEEE Commun. Lett., vol. 7, pp. 219-221, May 2003.

[9] B. Hu and N. C. Beaulieu, *"Accurate Evaluation of Multiple-Access Performance in TH-PPM and TH-BPSK UWB Systems"*, IEEE Trans. Commun., vol. 52, pp. 1758-1766 , Oct 2004.

[10] X. Huang and Y. Li *"Performances of Impulse Train Modulated Ultra-Wideband Systems"* , IEEE ICC-2002, Vol. 2, pp. 758-762, 2002.

[11] H. J. Landau and H. O. Pollak, *"Prolate Spheroidal Wave Functions, Fourier Analysis and Uncertainity-III: The Dimension of the Space of Essentially Time- and Band-limited Signals"* , B. S. T. J., 41, No. 4, pp. 1295-1336, Jul. 1962.

[12] P. G. Ciarlet, *"Introduction to numerical linear algebra and optimisation"* Cambridge University press, Cambridge, 1986.

[13] R. T. Rockafellar *"Convex Analysis"*, Princeton University Press, Princeton, 1970.

[14] D. Slepian and H. O. Pollak, *"Prolate Spheroidal Wave Functions, Fourier Analysis and Uncertainity-I"* , B. S. T. J., 40, pp. 43-64, Jan. 1961.

Appendix

Using the fact that $V = [\mathbf{p_1} \cdots \mathbf{p_m}]$, the set of inequalities in (18) can also be written as

$$-\mathbf{s} \leq [\mathbf{p_1} \quad \mathbf{p_2} \quad \cdots \quad \mathbf{p_m}]\mathbf{a} \leq \mathbf{s} \tag{21}$$

All the m columns of matrix V are independent as the columns $\mathbf{p_i}, i = \{1, \cdots, m\}$ are eigenvectors which have been proved to be independent. Hence, there will be m independent rows in V, say $\mathbf{r_1}, \cdots, \mathbf{r_m} \in \Re^{1\times m}$. Since $\mathbf{a} \in \Re^{m\times 1}$, $\mathbf{a}^t$ can be represented as the linear combination of m independent rows of V. From (21), $\mathbf{r_i a}$ is bounded for all $i = 1, \cdots, m$. Let $R = [\mathbf{r_1}^t, \cdots, \mathbf{r_m}^t]^t$ and $R\mathbf{a} = \mathbf{\Lambda}$. Since R is a $m \times m$ matrix with m independent rows, R^{-1} exists. Therefore, $\mathbf{a}$ can be expressed as $\mathbf{a} = R^{-1}\mathbf{\Lambda}$. As $\mathbf{\Lambda}$ is bounded, all the entries of $R^{-1}\mathbf{\Lambda}$ are also bounded. So, $\|\mathbf{a}\|$ is bounded.